COMPUTATIONAL STUDIES OF CONSERVED
MEAN-CURVATURE FLOW

Miroslav Kolář, Michal Beneš, Praha,

Daniel Ševčovič, Bratislava

Abstract. The paper presents the results of numerical solution of the evolution law for the constrained mean-curvature flow. This law originates in the theory of phase transitions for crystalline materials and describes the evolution of closed embedded curves with constant enclosed area. It is reformulated by means of the direct method into the system of degenerate parabolic partial differential equations for the curve parametrization. This system is solved numerically and several computational studies are presented as well.

Keywords: phase transitions; area-preserving mean-curvature flow; parametric method

MSC 2010: 35K57, 35K65, 65N40, 53C80

1. Introduction

The article deals with the non-local mean-curvature flow described by the evolution law

$$(1.1) \qquad v_\Gamma = -\kappa_\Gamma + \frac{1}{|\Gamma|} \int_\Gamma \kappa_\Gamma \, \mathrm{d}s,$$

$$\Gamma|_{t=0} = \Gamma_{\mathrm{ini}},$$

where Γ is a closed curve in $\mathbb{R}^2$, $\mathbf{n}_\Gamma$ the normal vector to Γ, v_Γ the velocity in the direction of the normal vector, κ_Γ the (mean) curvature of Γ and F the external prescribed force. Here $|\Gamma|$ is the length of Γ.

Problem (1.1) represents a variant of the mean curvature flow described as

(1.2)
$$v_\Gamma = -\kappa_\Gamma + F,$$
$$\Gamma|_{t=0} = \Gamma_{\text{ini}},$$

with a particular choice of the forcing term F, which has been widely studied in the literature (see e.g. [4]), as well as its various mathematical treatments by the direct (parametric) method (see e.g. [8], [14]), by the level-set method (see e.g. [15]) or by the phase-field method (see e.g. [2]).

The constrained motion by mean curvature has been discussed in the literature as well (see [7], [9], [10], [13]). In particular, problem (1.1) was mentioned in [5], [12], [16] within the context of a modification of the Allen-Cahn equation [1], [6] approximating the mean-curvature flow [2]. The non-local character of the equation is connected to the recrystallization phenomena where a fixed previously melted volume of the liquid phase solidifies again. It also can be applied in dislocation dynamics in crystalline materials or in the digital image processing (see e.g. [3]). In this text, we treat (1.1) by means of the parametric method and solve the resulting degenerate parabolic system numerically to provide the information on the solution behavior.

2. Equations

The direct method treating (1.1) considers parametrization of the smooth time-dependent curve $\Gamma(t)$ by means of the mapping

$$\vec{X} = \vec{X}(t, u), \quad u \in S^1,$$

where u is the parameter in a fixed interval. Here and after, we identify S^1 with the interval $[0, 1]$ and impose periodic boundary conditions on $\vec{X}$ at $u = 0, 1$. Consequently, the geometrical quantities of interest can be expressed by means of $\vec{X}$. The tangent vector and the normal vector are

$$\mathbf{t}_\Gamma = \frac{\partial_u \vec{X}}{|\partial_u \vec{X}|}, \quad \mathbf{n}_\Gamma = \frac{\partial_u \vec{X}^\perp}{|\partial_u \vec{X}|}.$$

The (mean) curvature is

(2.1)
$$\kappa_\Gamma = -\frac{1}{|\partial_u \vec{X}|} \partial_u \left(\frac{\partial_u \vec{X}}{|\partial_u \vec{X}|} \right) \cdot \mathbf{n}_\Gamma,$$

and the normal velocity in the direction of $\mathbf{n}_\Gamma$ (the projection of the point velocity $\vec{v}_\Gamma$ at Γ to $\mathbf{n}_\Gamma$) becomes

$$v_\Gamma = \vec{v}_\Gamma \cdot \mathbf{n}_\Gamma \quad \text{where } \vec{v}_\Gamma = \partial_t \vec{X}.$$

678

Substituting into (1.2) and assuming validity in the vectorial form yields the system

$$(2.2) \qquad \partial_t \vec{X} = \frac{1}{|\partial_u \vec{X}|} \partial_u \left(\frac{\partial_u \vec{X}}{|\partial_u \vec{X}|} \right) + F \frac{\partial_u \vec{X}^\perp}{|\partial_u \vec{X}|} \quad \text{in } (0, T) \times S^1$$

known as the parametric (direct) description of (1.2).

Among advantages of this approach, an easy and straightforward treatment of the curve dynamics without additional approximation is offered. On the other hand, topological changes are not captured by it.

Further modifications of (2.2) lead to the governing equation proposed by Dziuk et al. in [8] (see e.g. Beneš et al. [4] for applications in the dislocation dynamics)

$$(2.3) \qquad \partial_t \vec{X} = \frac{\partial_{uu} \vec{X}}{|\partial_u \vec{X}|^2} + F \frac{\partial_u \vec{X}^\perp}{|\partial_u \vec{X}|} \quad \text{in } (0, T) \times S^1$$

where

$$(2.4) \qquad F = \frac{1}{\int_{S^1} |\partial_u \vec{X}| \, \mathrm{d}u} \int_{S^1} \kappa_\Gamma(\vec{X}) |\partial_u \vec{X}| \, \mathrm{d}u$$

with $\kappa_\Gamma(\vec{X})$ given by (2.1), and the initial parametrization set as $\vec{X}|_{t=0} = \vec{X}_{\mathrm{ini}}$.

3. NUMERICAL SOLUTION

For the discretization of (2.2), the method of flowing finite volumes is used as e.g. in [4]. The discrete nodes $\vec{X}_i$, $i = 0, \dots, M$, are placed along $\Gamma(t)$ as shown in Figure 1. The governing equation is integrated along the dual segments surrounding
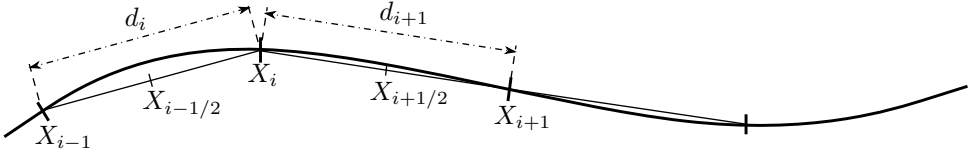

Figure 1. Curve discretization by finite volumes.

the nodes $\vec{X}_i$, $i = 1, \dots, M-1$:

$$\int_{u(X_{i-1/2})}^{u(X_{i+1/2})} \partial_t \vec{X} |\partial_u \vec{X}| \, \mathrm{d}u = \int_{u(X_{i-1/2})}^{u(X_{i+1/2})} \partial_u \left(\frac{\partial_u \vec{X}}{|\partial_u \vec{X}|} \right) \mathrm{d}u + F \int_{u(X_{i-1/2})}^{u(X_{i+1/2})} \partial_u \vec{X}^\perp \, \mathrm{d}u,$$

$$F = \frac{1}{\int_{S^1} |\partial_u \vec{X}| \, \mathrm{d}u} \int_{S^1} \kappa_\Gamma(\vec{X}) |\partial_u \vec{X}| \, \mathrm{d}u,$$

$$\kappa_\Gamma(\vec{X}) = -\frac{1}{|\partial_u \vec{X}|} \partial_u \left(\frac{\partial_u \vec{X}}{|\partial_u \vec{X}|} \right) \cdot \frac{\partial_u \vec{X}^\perp}{|\partial_u \vec{X}|}.$$

The resulting system of ordinary differential equations has the form

$$(3.1) \quad \frac{\mathrm{d}\vec{X}_i}{\mathrm{d}t} = \frac{2}{d_i + d_{i+1}} \left(\frac{\vec{X}_{i+1} - \vec{X}_i}{d_{i+1}} - \frac{\vec{X}_i - \vec{X}_{i-1}}{d_i} \right) + F \frac{(\vec{X}_{i+1}^{\perp} - \vec{X}_{i-1}^{\perp})}{d_i + d_{i+1}},$$

$$\kappa_i = \frac{2}{d_i + d_{i+1}} \left(\frac{\vec{X}_{i+1} - \vec{X}_i}{d_{i+1}} - \frac{\vec{X}_i - \vec{X}_{i-1}}{d_i} \right) \frac{(\vec{X}_{i+1}^{\perp} - \vec{X}_{i-1}^{\perp})}{d_i + d_{i+1}},$$

$$F = \frac{1}{\sum_{j=1}^{M} d_j} \sum_{j=1}^{M} \kappa_j \frac{d_{j+1} + d_j}{2},$$

$$d_i = |\vec{X}_i - \vec{X}_{i-1}|, \quad d_{M+1} := d_1, \quad \vec{X}_0 := \vec{X}_M, \quad \vec{X}_{M+1} := \vec{X}_1.$$

This system is solved by means of an semi-implicit backward Euler scheme. Details are similar to [3].

4. COMPUTATIONAL STUDIES

We use scheme (3.1) to perform a series of computational studies showing the behavior of the solution to (2.4) as the directly treated constrained mean-curvature flow

$$v_\Gamma = -\kappa_\Gamma + \frac{1}{|\Gamma|} \int_\Gamma \kappa_\Gamma \, \mathrm{d}s,$$

in comparison to the curve shortening flow

$$v_\Gamma = -\kappa_\Gamma.$$

The computations are analysed using the following measured quantity:

▷ Area enclosed by Γ, $A = \int_{\mathrm{Int}(\Gamma)} \mathrm{d}x$ should be preserved.

The following examples demonstrate how the solution of (2.4) evolves in time approaching the circular shape (called the Wulff shape), unlike the usual law (1.2) where the curve shrinks to a point when $F = 0$. In the examples, the discretization points remain almost uniformly distributed along the evolving curves during the considered evolution time intervals. No redistribution algorithm was necessary in this case (compare to [3], [14]).

E x a m p l e 1. In Figure 2, the first study shows the behavior of the solution when the initial four-folded curve is given by the formula

$$r_0(u) = 1 + 0.4 \cos(8\pi u), \quad u \in [0, 1].$$

The motion in the time interval $[0, 0.5]$ is driven by equation (1.2). The curve $\Gamma(t)$ asymptotically approaches the circular shape and shrinks to a point in finite time (compare with [11], [17]). The number of finite volumes is $M = 200$.
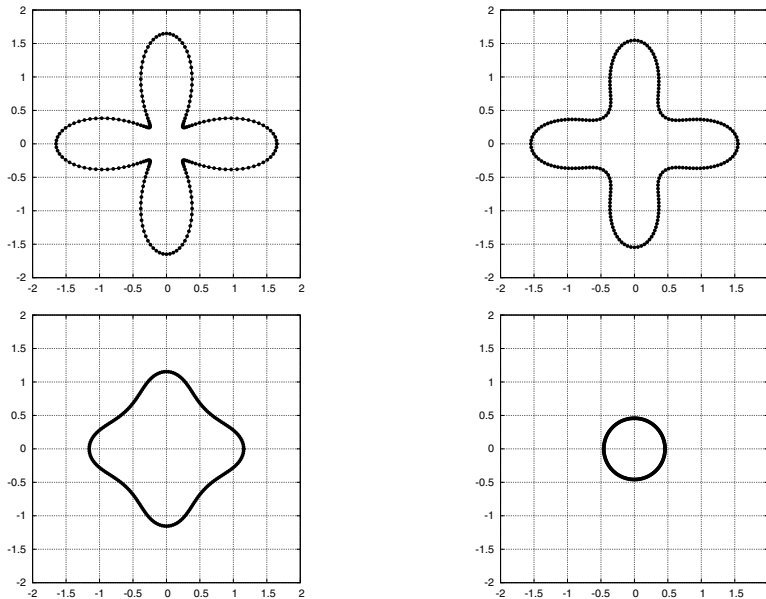
Figure 2. Curve shortening flow (1.2) for which any closed curve shrinks to a point—the curve $\Gamma(t)$ is depicted for $t = 0$, $t = 0.025$, $t = 0.125$ and $t = 0.5$.

E x a m p l e 2. In Figure 3, the second study shows the behavior of the solution when the initial five-folded curve is given by the formula

$$r_0(u) = 1 + 0.65 \cos(10\pi u), \quad u \in [0, 1].$$

The motion in the time interval $[0, 0.5]$ is driven by equation (1.1). The curve $\Gamma(t)$ asymptotically approaches the circular shape whereas the enclosed area is preserved (see [16]). The number of finite volumes is $M = 200$. The initial curve encloses the area of 3.839 and at $t = 0.5$, the curve encloses the area of 3.834.

E x a m p l e 3. In Figure 4, the third study shows the behavior of the solution when the initial ten-folded curve is given by the formula

$$r_0(u) = 1 + 0.45 \cos(20\pi u), \quad u \in [0, 1].$$

The motion in the time interval $[0, 0.5]$ is driven by equation (1.1). The curve $\Gamma(t)$ asymptotically approaches the circular shape whereas the enclosed area is preserved (see [16]). The number of finite volumes is $M = 200$. The initial curve encloses the area of 3.476 and at $t = 0.5$, the curve encloses the area of 3.470.
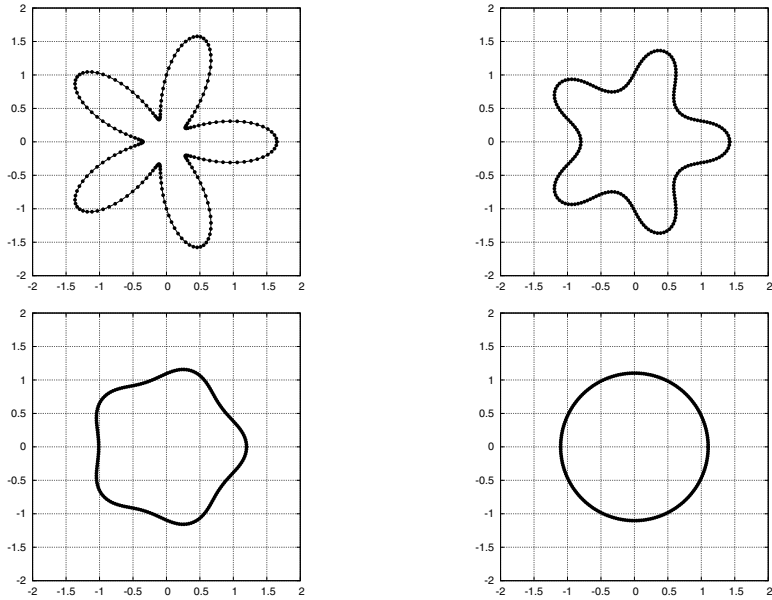
Figure 3. Area-preserving mean curvature flow (1.1) where the initial 5-folded curve asymptotically attains the circular shape. The curve $\Gamma(t)$ is depicted for $t = 0$, $t = 0.05$, $t = 0.125$ and $t = 0.5$.
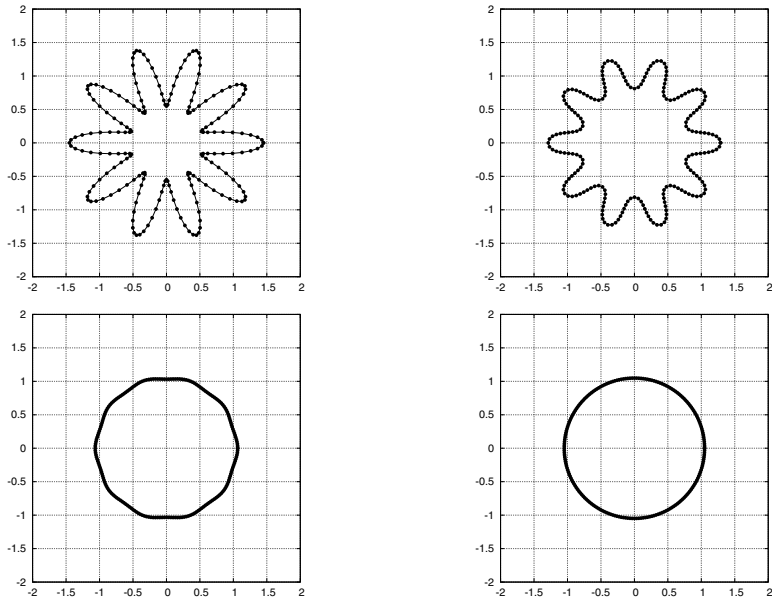

Figure 4. Area-preserving mean curvature flow (1.1) where the initial 10-folded curve asymptotically attains the circular shape. The curve $\Gamma(t)$ is depicted for $t = 0$, $t = 0.0125$, $t = 0.05$ and $t = 0.5$.

E x a m p l e 4. In Figure 5, the fourth study shows the behavior of the solution for the initial π-shaped curve whose parametric equations can be found in the Wolfram Alpha Database (`http://www.wolframalpha.com`). The motion in the time interval $[0, 1.25]$ is driven by problem (1.1). The curve $\Gamma(t)$ asymptotically approaches the circular shape whereas the enclosed area is preserved (see [16]). The number of finite volumes is $M = 200$. The initial curve encloses the area of 20.61 and at $t = 1.25$, the curve encloses the area of 20.53.
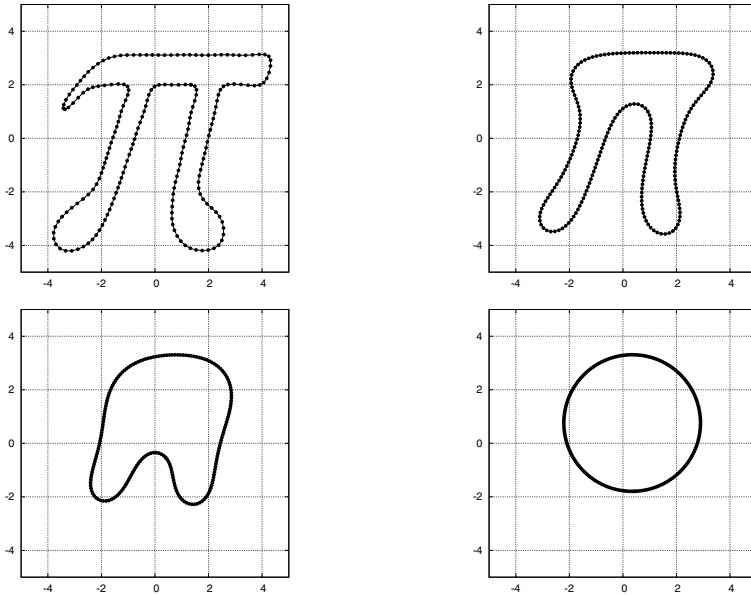

Figure 5. Area-preserving mean curvature flow (1.1) where the initial π-shaped curve asymptotically attains the circular shape. The curve $\Gamma(t)$ is depicted for $t = 0$, $t = 0.05$, $t = 0.125$ and $t = 1.25$.

5. Conclusion

The paper studies the area-preserving mean curvature flow in the terms of qualitative behavior of the solution obtained numerically. The studies confirmed the theoretical indications that the solution approaches the circular shape in long term (see [10], [16]). This behavior corresponds to the expected use in modeling the recrystallization phenomena in solid phase.

References

[1] *S. Allen, J. Cahn*: A microscopic theory for antiphase boundary motion and its application to antiphase domain coarsening. Acta Metall. *27* (1979), 1084–1095.

[2] *M. Beneš*: Diffuse-interface treatment of the anisotropic mean-curvature flow. Mathematical and computer modeling in science and engineering. Appl. Math., Praha *48* (2003), 437–453. zbl MR

[3] *M. Beneš, M. Kimura, P. Pauš, D. Ševčovič, T. Tsujikawa, S. Yazaki*: Application of a curvature adjusted method in image segmentation. Bull. Inst. Math., Acad. Sin. (N.S.) *3* (2008), 509–523. zbl MR

[4] *M. Beneš, J. Kratochvíl, J. Křišťan, V. Minárik, P. Pauš*: A parametric simulation method for discrete dislocation dynamics. European Phys. J. ST *177* (2009), 177–192.

[5] *M. Beneš, S. Yazaki, M. Kimura*: Computational studies of non-local anisotropic Allen-Cahn equation. Math. Bohem. *136* (2011), 429–437. zbl MR

[6] *J. W. Cahn, J. E. Hilliard*: Free energy of a nonuniform system. III. Nucleation of a two-component incompressible fluid. J. Chem. Phys. *31* (1959), 688–699.

[7] *I. Capuzzo Dolcetta, S. Finzi Vita, R. March*: Area-preserving curve-shortening flows: From phase separation to image processing. Interfaces Free Bound. *4* (2002), 325–343. zbl MR

[8] *K. Deckelnick, G. Dziuk, C. M. Elliott*: Computation of geometric partial differential equations and mean curvature flow. Acta Numerica *14* (2005), 139–232. zbl MR

[9] *S. Esedoḡlu, S. J. Ruuth, R. Tsai*: Threshold dynamics for high order geometric motions. Interfaces Free Bound. *10* (2008), 263–282. zbl MR

[10] *M. Gage*: On an area-preserving evolution equation for plane curves. Nonlinear Problems in Geometry, Proc. AMS Spec. Sess., Mobile/Ala. 1985 (D. M. DeTurck, ed.). Contemp. Math. 51, American Mathematical Society, Providence, 1986, pp. 51–62. zbl MR

[11] *M. A. Grayson*: The heat equation shrinks embedded plane curves to round points. J. Differ. Geom. *26* (1987), 285–314. zbl MR

[12] *M. Henry, D. Hilhorst, M. Mimura*: A reaction-diffusion approximation to an area preserving mean curvature flow coupled with a bulk equation. Discrete Contin. Dyn. Syst., Ser. S *4* (2011), 125–154. zbl MR

[13] *J. McCoy*: The surface area preserving mean curvature flow. Asian J. Math. *7* (2003), 7–30. zbl MR

[14] *V. Minárik, M. Beneš, J. Kratochvíl*: Simulation of dynamical interaction between dislocations and dipolar loops. J. Appl. Phys. *107* (2010), Article No. 061802, 13 pages.

[15] *S. Osher, J. A. Sethian*: Fronts propagating with curvature-dependent speed: Algorithms based on Hamilton-Jacobi formulations. J. Comput. Phys. *79* (1988), 12–49. zbl MR

[16] *J. Rubinstein, P. Sternberg*: Nonlocal reaction-diffusion equations and nucleation. IMA J. Appl. Math. *48* (1992), 249–264. zbl MR

[17] *D. Ševčovič*: Qualitative and quantitative aspects of curvature driven flows of planar curves. Topics on Partial Differential Equations (P. Kaplický et al., eds.). Jindřich Nečas Center for Mathematical Modeling Lecture Notes 2, Matfyzpress, Praha, 2007, pp. 55–119. zbl MR

Authors' addresses: *Miroslav Kolář*, *Michal Beneš*, Faculty of Nuclear Sciences and Physical Engineering Czech Technical University in Prague, Břehová 7, 115 19 Praha 1, Czech Republic, e-mail: `kolarmir@fjfi.cvut.cz`, `michal.benes@fjfi.cvut.cz`; *Daniel Ševčovič*, Comenius University, Faculty of Mathematics and Physics, Institute of Applied Mathematics, Mlynská dolina 15, 842 48 Bratislava, Slovakia, e-mail: `sevcovic@fmph.uniba.sk`.